Published in final edited form as:
Cell Rep. 2013 March 28; 3(3): 646–650. doi:10.1016/j.celrep.2013.02.016.

Induced Pluripotent Stem Cell-Derived Neural Cells Survive and Mature in the Nonhuman Primate Brain

Marina E. Emborg[1,2,6], **Yan Liu**[3,6], **Jiajie Xi**[3], **Xiaoqing Zhang**[3], **Yingnan Yin**[3], **Jianfeng Lu**[3], **Valerie Joers**[1], **Christine Swanson**[1], **James E. Holden**[1,2], and **Su-Chun Zhang**[3,4,5,*]

[1]Preclinical Parkinson's Research Program, Wisconsin National Primate Research Center, University of Wisconsin, Madison, WI 53705, USA

[2]Department of Medical Physics, University of Wisconsin, Madison, WI 53705, USA

[3]Waisman Center, University of Wisconsin, Madison, WI 53705, USA

[4]Department of Neuroscience, University of Wisconsin, Madison, WI 53705, USA

[5]Department of Neurology School of Medicine and Public Health, University of Wisconsin, Madison, WI 53705, USA

SUMMARY

The generation of induced pluripotent stem cells (iPSCs) opens up the possibility for personalized cell therapy. Here, we show that transplanted autologous rhesus monkey iPSC-derived neural progenitors survive for up to 6 months and differentiate into neurons, astrocytes, and myelinating oligodendrocytes in the brains of MPTP-induced hemiparkinsonian rhesus monkeys with a minimal presence of inflammatory cells and reactive glia. This finding represents a significant step toward personalized regenerative therapies.

INTRODUCTION

Autologous transplantation via induced pluripotent stem cells (iPSCs) is a potential strategy for having readily available matching donor cells and therefore minimizing host immune response (Okita and Yamanaka, 2011). A recent study showed rejection of iPSC-derived teratomas by syngenic host mice (Zhao et al., 2011), casting doubt on the utility of reprogrammed cells for autologous transplant therapy. To explore the utility and feasibility of the iPSC strategy as an autologous cell therapy in a preclinical setting, we derived iPSCs from the skin tissue of three rhesus monkeys (aged 8–10 years) using retrovirus containing the same reprogramming human genes (*oct4*, *sox2*, *klf4*, and *myc*) employed by Yamanaka and colleagues (Takahashi et al., 2007). These iPSCs exhibited characteristic primate embryonic stem cell (ESC) morphology and expressed pluripotent proteins, including SOX2 and NANAOG (Figures S1A–S1D), similar to rhesus ESCs (Thomson et al., 1995) and iPSCs (Liu et al., 2008; Deleidi et al., 2011). They generated teratomas after being injected into severe combined immunodeficiency (SCID) mice (Figure S1J).

*Correspondence: zhang@waisman.wisc.eduhttp://dx.doi.org/10.1016/j.celrep.2013.02.016.
[6]These authors contributed equally to this work

SUPPLEMENTAL INFORMATION Supplemental Information includes two figures and two tables and can be found with this article online at http://dx.doi.org/10.1016/j.celrep.2013.02.016.

RESULTS

The rhesus iPSCs were differentiated into neuroepithelia and then neurons and glia according to our established protocol for primate PSCs (Pankratz et al., 2007). We biased the cells toward a dopaminergic fate using a protocol modified from the traditional method (Perrier et al., 2004; Yan et al., 2005; Cooper et al., 2010) with an attempt to examine the dopaminergic differentiation potential (Figure 1A). Similar to human PSCs (hPSCs), rhesus iPSCs differentiated to neuroepithelia that organized into neural tube-like rosettes and expressed neuroectoderm transcription factors Pax6 and Sox1 under a chemically defined medium without the presence of exogenous growth factors in 10–14 days (Figure 1C). The neural rosettes were expanded in the presence of sonic hedgehog (SHH, C-24/25, R&D Systems, 200–500 ng/ml) and fibroblast growth factor 8 (FGF8, 100 ng/ml) for the following 2 weeks before being differentiated into neurons on a laminin substrate (Yan et al., 2005). By day 42, the time for cell transplantation, 37% of the cells were bIII-tubulin$^+$ neurons, 16% were S-100b$^+$ immature astrocytes, and the remaining were largely nestin$^+$ progenitors (Figures 1B and 1C). No O4$^+$ oligodendrocytes were observed at this stage, which usually appear at a much later stage during primate stem cell differentiation (Hu et al., 2009). The major neuronal populations were positive for g-butyric acid (GABA, 49%) and tyrosine hydroxylase (TH, 16%) (Figures 1B and 1C). Among the TH$^+$ neurons, 87% expressed a floor plate marker FOXA2 and 64% were positive for the A10 marker Calbindin, whereas most TH$^+$ neurons also expressed the A9 marker Girk2 (Figures S1G–S1I).

To examine the survival and differentiation of iPSC-derived neural cells in the primate brain, we created a monkey model of Parkinson's disease by unilateral intracarotid artery infusion of the neurotoxin 1-methyl-4-phenyl-1,2,3,6,-tetrahydropyridine (MPTP) (Emborg et al., 2008). All the three monkeys developed a stable hemiparkinsonian condition, characterized by slight tremors, bradykinesia (slowness of movement), postural and gait imbalance, as well as impairment in gross and fine motor skills in the hand contralateral to the MPTP injection side, as measured by a clinical rating scale (CRS) (Emborg et al., 2009) and confirmed by ^{11}C-dihydrotetrabenazine (DTBZ) positron emission tomography (PET) 12–18 months after the neurotoxin infusion.

In order to identify the autologous transplants in the host brain, we first established iPSC lines that carry GFP under the phosphoglycerate kinase (PGK) promoter through lentivirus infection and cloning (Figure S1E). Since reporter genes under ubiquitous promoters tend to be downregulated after primate PSC differentiation to mature neurons even though the transgenes are mostly retained in progenitors and glia (Xia et al., 2007), we labeled the rhesus neural progenitors at day 30 via infection with lentivirus carrying the synapsin promoter driving GFP. Cells at the time of transplantation (day 42), including immature neurons, were largely positive for GFP (Figure S1F). To avoid potential overgrowth and to test potential immunological rejection, we chose cells that were differentiated for 42 days, a stage commonly used for transplantation into rodent models (Yang et al., 2008; Deleidi et al., 2011; Hargus et al., 2010), and transplanted into the striatum and substantia nigra of the same monkeys 12–18 months post-MPTP lesion without any immune suppression. Cultures at that stage contained both postmitotic neurons and dividing progenitors (Figure 1B).

Previous studies indicate that hPSC-derived neural transplants into parkinsonian rhesus monkeys were rejected within 3 months even under daily dosing of cyclosporine (Emborg et al., 2012). A recent study also showed that hPSC-derived neural grafts were filled with infiltrating cells by 1 month (Kriks et al., 2011). We therefore examined the grafts 6 months posttransplantation using stereological analysis on serial coronal sections (Emborg et al., 2009). Examination under a bright field or with Nissl staining revealed normal striatal and

nigral cytoarchitecture; the grafts were not readily discernible in any of the monkeys (Figures 1D and S2). However, after immunostaining for GFP or viewing under a fluorescent microscope, discrete grafts were present in the striatum and substantia nigra of all the grafted monkeys, ranging from 1.36 to 160.50 mm^2 (Figures S1 and S2; Table S1). Stereological cell counts showed that there were 11,556, 26,655 and 34,321 GFP^+ cells in the three monkeys, respectively (Table S1). The total cell numbers may be underestimated as GFP expression may be downregulated in some of the grafted cells, especially neurons.

Analysis of the GFP^+ cells indicated that about 63% were $MAP2^+$ neurons, 22% were $GFAP^+$ astrocytes, and approximately 10% were myelin basic protein $(MBP)^+$ oligodendrocytes (Figures 1E and 1F). Most of the GFP^+ neurons were located in the graft, and the GFP fibers extended into the surrounding host tissue for up to 1.5 mm in one direction. Individual neurons were also present outside of the graft, expressing Tuj1, MAP2, and NeuN (Figure 1F), suggestive of maturation. The vast majority of the GFP^+ neurons were $GABA^+$ and few were positive for TH (Figure 1F). This may explain why we did not observe obvious behavioral recovery and PET changes (data not shown). $GFAP^+$ astrocytes were present both in and outside of the graft, exhibiting filamentous morphology (Figures 1F and 2),indistinguishable from endogenous astrocytes without GFP marking. MBP^+ oligodendrocytes were localized mainly to the surrounding of the graft, exhibiting bush-like morphology. Some of the GFP fibers colabeled with MBP (Figure 1F), suggestive of myelination. In this case, the cell bodies were not labeled. Therefore, the proportion of oligodendrocytes is underestimated. Immunostaining for Ki67, labeling mitotic cells, showed no positive cells in the grafts (data not shown), indicating differentiation of grafted progenitors. No cells were positive for OCT4, NANOG, SOX17, or Brachyury in the grafted brain, indicating the absence of pluripotent stem cells and cells of nonneural lineages. These results indicate that almost all the grafted cells become neurons, astrocytes, and oligodendrocytes, at least based on the GFP-labeled population. They also indicate that overgrowth or tumorigenicity, a major concern of PSC-based cell therapy, is not present in the present setting.

Human ESC-derived neural grafts in monkeys (Kriks et al., 2011) as well as teratomas in syngenic mice (Zhao et al., 2011) were infiltrated with lymphocytes and microglia/macrophages by 1 month when the animals were sacrificed. Immunostaining for CD3 and CD8 (for lymphocytes) on our monkey brain sections showed no obvious difference between the graft and surrounding host tissues (Figures 2 and S2), whereas the brain tissue transplanted with human ESC-derived neural cells (Emborg et al., 2012) as well as spleen tissues (used as positive controls) were immunoreactive for all the markers. The lack of lymphocyte infiltration suggests the absence of immune response. Immunostaining for human leukocyte antigen D-related (HLA-DR, for microglia and macrophages) revealed microglial cells throughout the brain, and the microglial cells in and surrounding the graft exhibited a largely ramified morphology (Figures 2 and S2). However, there was a mild increase in the intensity of HLA-DR staining in the grafts and surroundings, possibly due to MPTP toxicity and/or physical damage during transplantation. Immunostaining for general GFAP showed a moderate increase in the intensity (Figure 2). The increased staining, especially in the graft, is partially due to the accumulation of $GFAP^+$ astrocytes that were differentiated from grafted progenitors, as shown by GFP labeling (Figures 2 and S2). Besides the response to MPTP toxicity and physical (transplant) damages, the mild to moderate increase in the intensity of HLA-DR and GFAP staining may represent glial response to the graft that has not yet functionally integrated in the host brain.

DISCUSSION

Cell therapy is one potential future application of stem cells, especially of iPSCs, given the possibility of autologous transplantation (Brundin et al., 2010; Redmond et al., 2010; Deleidi et al., 2011). Although teratomas are rejected by syngenic mice, stem cell therapy will unlikely employ iPSCs themselves. Instead, differentiated progenies of stem cells will be used, as exemplified here. Our results indicate that the autologous iPSC-derived neural cell transplants in the primate brain are not rejected, as opposed to the immunological rejection of teratomas by syngenic mice (Zhao et al., 2011). There is no infiltration of blood-borne cells (macrophages and lymphocytes) and little response of endogenous glia (astrocytes and microglia), suggesting that one reason for lymphocyte infiltration and rejection in the syngenic iPSC transplantation (Zhao et al., 2011) is toward tumor formation and/or pluripotent proteins. The iPSC-derived neural progenitors survive and produce mature neurons, astrocytes, and oligodendrocytes in the monkey brain. Importantly, the grafted neural cells appear to structurally integrate into the host brain as we barely discerned the grafts unless by genetic marking, and the differentiated neurons extend long processes and the oligodendrocytes participate in myelination.

The present finding, though from limited numbers of non-human primates, provides proof of principle that iPSC derivatives can engraft and survive in the primate brain, raising hopes for cell therapy employing human stem cells. The graft size, however, is relatively small. This may be due to the following reasons. First, we used relatively mature cells (differentiated for 42 days), which contain over 50% of postmitotic cells. This is a stage that is commonly used for transplantation into rodent models (Yang et al., 2008; Deleidi et al., 2011; Hargus et al., 2010) and that has recently been shown to be relatively safe in transplanting into the monkey brain (Doi et al., 2012). However, this could reduce the survival rate of postmitotic cells, especially TH^+ neurons, during and after transplantation into the monkey brain. Second, we used suspension of individual cells instead of tissue chunks (Freed et al., 2001; Olanow et al., 2003) or cell suspension with cell aggregates (Mendez et al., 2005) that are typically used for transplantation in human and nonhuman primates, thus further compromising the survival. The choice of dissociated individual cells was designed for easy standardization for future application. Third, the number of grafted cells, especially neurons, is likely underestimateddue to inherent problems relating to random insertion of lentivirus and downregulation of the reporter gene along neuronal differentiation. This technical issue may now be overcome by the newly developed TALEN (transcription activator-like effector nucleases) technique to insert a reporter into one of the envy sites (Hockemeyer et al., 2011) so that the transgene may be maintained after differentiation. This will allow more accurate quantification of autologously grafted cells. The above potential reasons behind the small graft size may form the basis for experimental design for future preclinical studies.

Despite small graft size, the grafted neurons do project axons over a long distance even under the adult brain environment, oligodendrocytes produce myelin sheaths, and glial response is minimal. The scarcity of dopamine neurons in the grafts and lack of functional improvement in the animals are likely due to the neural differentiation strategy that does not yield sufficient numbers of midbrain dopamine neurons besides the reasons described above. Recently, we (Xi et al., 2012), as well as others (Kriks et al., 2011; Kirkeby et al., 2012), have developed an efficient strategy for differentiating primate ESCs and iPSCs to authentic midbrain dopamine neurons, which will allow us to evaluate individualized cell therapy in the primate model at the functional level for a longer term.

EXPERIMENTAL PROCEDURES

This study was performed in strict accordance with the recommendations in the Guide for the Care and Use of Laboratory Animals of the NIH (1996) in an AAALAC-accredited facility (University of Wisconsin-Madison).

iPSC Generation and Neural Differentiation

A cylindrical sample of skin and subcutaneous tissue was obtained from each of the three adult female *macaca mulatta* monkeys (8–10 years old), and fibroblasts were cultured in DMEM with 10% fetal bovine serum (Hu et al., 2010). iPSCs (six lines for each monkey) were generated by infecting 1 3 10^5 fibroblasts with retroviruses expressing Oct3/4, Sox2, Klf4, and c-Myc (Takahashi et al., 2007). The pluripotency was tested by teratoma assay (Hu et al., 2010).

For dopamine neuron generation, primitive neuroepithelia at day 10 of iPSC differentiation were treated with SHH (C-24/25, R&D, 200 ng/ml) and FGF8 (R&D, 100 ng/ml) from days 14–28 (Yan et al., 2005). The neural progenitors were then cultured on a laminin substrate in low SHH (50 ng/ml) and FGF8 (50 ng/ml) until day 42 for immunocytochemical analysis and transplantation (Yang et al., 2008).

MPTP Model and Cell Transplantation

The parkinsonism was induced by intracarotid artery infusion of MPTP, and the parkinsonian state was evaluated by CRS and 11C-DTBZ PET (Swanson et al., 2011). Twelve to 18 months later, the animals received six MRI-guided stereo-taxic injections of autologous iPSC-derived cell suspensions (50,000 cells/ml) into the precommisural (10 ml) and commissural (5 ml) caudate nucleus, the pre-commisural (10 ml), commissural (10 ml) and postcommisural (10 ml) putamen, and the substantia nigra (5 ml) ipsilateral to the MPTP injection. The animals were sacrificed 6 months postgrafting (Swanson et al., 2011).

Immunohistochemical Characterization of Cultured Cells and the Grafts

Immunofluorescent staining and cellular quantification for coverslip cultures and free-floating monkey brain sections were performed as described (Yang et al., 2008) along with spleen tissues as positive controls for blood-borne cells. The stereological analysis of the grafts on serial cross-sections stained for GFP using the diaminobenzidine method with Nissl counterstaining was detailed elsewhere (Swanson et al., 2011). The primary antibodies were listed in Table S2.

Supplementary Material

Refer to Web version on PubMed Central for supplementary material.

Acknowledgments

This study was supported in part by NIH-NINDS (NS045926 and NS076352), the Parkinson's Disease Foundation, Center for Stem Cells and Regenerative Medicine at the University of Wisconsin Madison, the NICHD (P30 HD03352), NIH-NCRR grant P51 RR000167 (Wisconsin National Primate Research Center), and the Schmal Family Trust. This research was conducted at a facility constructed with support from Research Facilities Improvement Program grants RR15459-01 and RR020141-01. The authors are grateful to Nichole Goecks, Victoria Carter, Viktorya Bondarenko, and Rebecca Velotta for excellent technical assistance, Dr. Sachiko Ohshima for surgical assistance and Dr. Kevin Brunner for expert veterinarian support.

REFERENCES

Brundin P, Barker RA, Parmar M. Neural grafting in Parkinson's disease Problems and possibilities. Prog. Brain Res. 2010; 184:265–294. [PubMed: 20887880]

Cooper O, Hargus G, Deleidi M, Blak A, Osborn T, Marlow E, Lee K, Levy A, Perez-Torres E, Yow A, Isacson O. Differentiation of human ES and Parkinson's disease iPS cells into ventral midbrain dopaminergic neurons requires a high activity form of SHH, FGF8a and specific regionalization by retinoic acid. Mol. Cell. Neurosci. 2010; 45:258–266. [PubMed: 20603216]

Deleidi M, Hargus G, Hallett P, Osborn T, Isacson O. Development of histocompatible primate-induced pluripotent stem cells for neural transplantation. Stem Cells. 2011; 29:1052–1063. [PubMed: 21608081]

Doi D, Morizane A, Kikuchi T, Onoe H, Hayashi T, Kawasaki T, Motono M, Sasai Y, Saiki H, Gomi M, et al. Prolonged maturation culture favors a reduction in the tumorigenicity and the dopaminergic function of human ESC-derived neural cells in a primate model of Parkinson's disease. Stem Cells. 2012; 30:935–945. [PubMed: 22328536]

Emborg ME, Ebert AD, Moirano J, Peng S, Suzuki M, Capowski E, Joers V, Roitberg BZ, Aebischer P, Svendsen CN. GDNF-secreting human neural progenitor cells increase tyrosine hydroxylase and VMAT2 expression in MPTP-treated cynomolgus monkeys. Cell Transplant. 2008; 17:383–395. [PubMed: 18522241]

Emborg ME, Moirano J, Raschke J, Bondarenko V, Zufferey R, Peng S, Ebert AD, Joers V, Roitberg B, Holden JE, et al. Response of aged parkinsonian monkeys to in vivo gene transfer of GDNF. Neurobiol. Dis. 2009; 36:303–311. [PubMed: 19660547]

Emborg, ME.; Zhang, Z.; Joers, VM.; Brunner, K.; Bondarenko, V.; Ohshima, S.; Zhang, SC. Intracerebral transplantation of differentiated human embryonic stem cells to hemiparkinsonian monkeys. Cell Transplant. 2012. Published online June 15, 2012. http://dx.doi.org/10.3727/096368912X47144

Freed CR, Greene PE, Breeze RE, Tsai WY, DuMouchel W, Kao R, Dillon S, Winfield H, Culver S, Trojanowski JQ, et al. Transplantation of embryonic dopamine neurons for severe Parkinson's disease. N. Engl. J. Med. 2001; 344:710–719. [PubMed: 11236774]

Hargus G, Cooper O, Deleidi M, Levy A, Lee K, Marlow E, Yow A, Soldner F, Hockemeyer D, Hallett PJ, et al. Differentiated Parkinson patient-derived induced pluripotent stem cells grow in the adult rodent brain and reduce motor asymmetry in Parkinsonian rats. Proc. Natl. Acad. Sci. USA. 2010; 107:15921–15926. [PubMed: 20798034]

Hockemeyer D, Wang H, Kiani S, Lai CS, Gao Q, Cassady JP, Cost GJ, Zhang L, Santiago Y, Miller JC, et al. Genetic engineering of human pluripotent cells using TALE nucleases. Nat. Biotechnol. 2011; 29:731–734. [PubMed: 21738127]

Hu BY, Du ZW, Li XJ, Ayala M, Zhang SC. Human oligodendrocytes from embryonic stem cells: conserved SHH signaling networks and divergent FGF effects. Development. 2009; 136:1443–1452. [PubMed: 19363151]

Hu BY, Weick JP, Yu J, Ma LX, Zhang XQ, Thomson JA, Zhang SC. Neural differentiation of human induced pluripotent stem cells follows developmental principles but with variable potency. Proc. Natl. Acad. Sci. USA. 2010; 107:4335–4340. [PubMed: 20160098]

Kirkeby A, Grealish S, Wolf DA, Nelander J, Wood J, Lundblad M, Lindvall O, Parmar M. Generation of regionally specified neural progenitors and functional neurons from human embryonic stem cells under defined conditions. Cell Rep. 2012; 1:703–714. [PubMed: 22813745]

Kriks S, Shim JW, Piao J, Ganat YM, Wakeman DR, Xie Z, Carrillo-Reid L, Auyeung G, Antonacci C, Buch A, et al. Dopamine neurons derived from human ES cells efficiently engraft in animal models of Parkinson's disease. Nature. 2011; 480:547–551. [PubMed: 22056989]

Liu H, Zhu F, Yong J, Zhang P, Hou P, Li H, Jiang W, Cai J, Liu M, Cui K, et al. Generation of induced pluripotent stem cells from adult rhesus monkey fibroblasts. Cell Stem Cell. 2008; 3:587–590. [PubMed: 19041774]

Mendez I, Sanchez-Pernaute R, Cooper O, Viñuela A, Ferrari D, Björklund L, Dagher A, Isacson O. Cell type analysis of functional fetal dopamine cell suspension transplants in the striatum and substantia nigra of patients with Parkinson's disease. Brain. 2005; 128:1498–1510. [PubMed: 15872020]

Okita K, Yamanaka S. Induced pluripotent stem cells: opportunities and challenges. Philos. Trans. R. Soc. Lond. B Biol. Sci. 2011; 366:2198–2207. [PubMed: 21727125]

Olanow CW, Goetz CG, Kordower JH, Stoessl AJ, Sossi V, Brin MF, Shannon KM, Nauert GM, Perl DP, Godbold J, Freeman TB. A double-blind controlled trial of bilateral fetal nigral transplantation in Parkinson's disease. Ann. Neurol. 2003; 54:403–414. [PubMed: 12953276]

Pankratz MT, Li XJ, Lavaute TM, Lyons EA, Chen X, Zhang SC. Directed neural differentiation of human embryonic stem cells via an obligated primitive anterior stage. Stem Cells. 2007; 25:1511–1520. [PubMed: 17332508]

Perrier AL, Tabar V, Barberi T, Rubio ME, Bruses J, Topf N, Harrison NL, Studer L. Derivation of midbrain dopamine neurons from human embryonic stem cells. Proc. Natl. Acad. Sci. USA. 2004; 101:12543–12548. [PubMed: 15310843]

Redmond DE Jr. Weiss S, Elsworth JD, Roth RH, Wakeman DR, Bjugstad KB, Collier TJ, Blanchard BC, Teng YD, Synder EY, Sladek JR Jr. Cellular repair in the parkinsonian nonhuman primate brain. Rejuvenation Res. 2010; 13:188–194. [PubMed: 20370501]

Swanson CR, Joers V, Bondarenko V, Brunner K, Simmons HA, Ziegler TE, Kemnitz JW, Johnson JA, Emborg ME. The PPAR-g agonist pioglitazone modulates inflammation and induces neuroprotection in parkinsonian monkeys. J. Neuroinflammation. 2011; 8:91. [PubMed: 21819568]

Takahashi K, Tanabe K, Ohnuki M, Narita M, Ichisaka T, Tomoda K, Yamanaka S. Induction of pluripotent stem cells from adult human fibroblasts by defined factors. Cell. 2007; 131:861–872. [PubMed: 18035408]

Thomson JA, Kalishman J, Golos TG, Durning M, Harris CP, Becker RA, Hearn JP. Isolation of a primate embryonic stem cell line. Proc. Natl. Acad. Sci. USA. 1995; 92:7844–7848. [PubMed: 7544005]

Xi J, Liu Y, Liu H, Chen H, Emborg ME, Zhang SC. Specification of midbrain dopamine neurons from primate pluripotent stem cells. Stem Cells. 2012; 30:1655–1663. [PubMed: 22696177]

Xia X, Zhang Y, Zieth CR, Zhang SC. Transgenes delivered by lentiviral vector are suppressed in human embryonic stem cells in a promoter-dependent manner. Stem Cells Dev. 2007; 16:167–176. [PubMed: 17348812]

Yan Y, Yang D, Zarnowska ED, Du Z, Werbel B, Valliere C, Pearce RA, Thomson JA, Zhang SC. Directed differentiation of dopaminergic neuronal subtypes from human embryonic stem cells. Stem Cells. 2005; 23:781–790. [PubMed: 15917474]

Yang D, Zhang ZJ, Oldenburg M, Ayala M, Zhang SC. Human embryonic stem cell-derived dopaminergic neurons reverse functional deficit in parkinsonian rats. Stem Cells. 2008; 26:55–63. [PubMed: 17951220]

Zhao T, Zhang ZN, Rong Z, Xu Y. Immunogenicity of induced pluripotent stem cells. Nature. 2011; 474:212–215. [PubMed: 21572395]

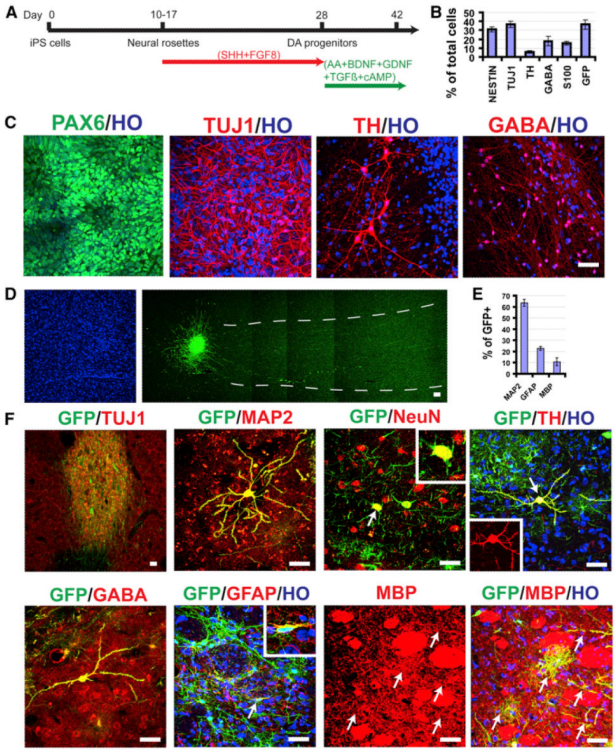

Figure 1. Differentiation of Grafted Neural Progenitors

(A) Schematic diagram of iPSC differentiation to neural progenitors and dopaminergic neurons.

(B) Quantification of cell populations at day 42 (the day for transplantation).

(C) On day 14, neuroepithelia organize into rosettes and express Pax6. By day 42, most cells express Tuj1, and some are positive for TH and GABA.

(D) Six months posttransplantation, Hoechst-labeled nuclei and corresponding GFP-labeled graft in the putamen show nondisrupted cytoarchitecture of the grafted area as well as the graft and cellular projections.

(E) Quantification of neurons ($MAP2^+$), astrocytes ($GFAP^+$), and oligodendrocytes (MBP^+) among GFP^+ grafted cells.

(F) Colabeling of GFP with neuronal (Tuj1, MAP2, NeuN, TH, GABA) and glial (GFAP, MBP) markers in the graft. HO, Hoechst. The bar represents 50 mm.

Data are presented as mean ± SE. See also Figure S1.

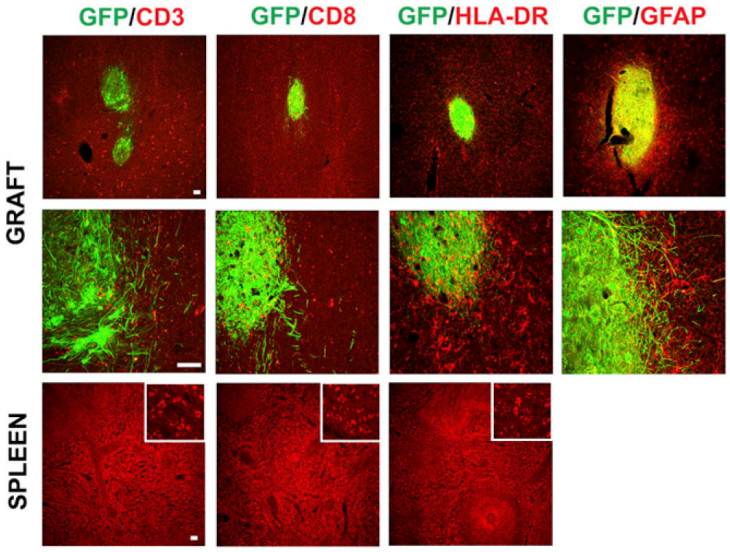

Figure 2. Reaction of Glia and Infiltration of Leukocytes in the Grafts

Shown are representatives of grafts in the putamen revealed by GFP. These sections are colabeled with antibodies against HLA-DR (for microglia and macrophages), CD3 and CD8 (for lymphocytes), as well as GFAP (for astrocytes). Lower row is the spleen tissue sections as positive controls for HLA-DR, CD3, and CD8. HO, Hoechst. The bar represents 50 mm. See also Figure S2.